Effects of phase noise in an optical six-port measurement technique

I. Molina-Fernández, J. de-Oliva-Rubio

Departamento de Ingeniería de Comunicaciones, E.T.S.I. Telecomunicación, Málaga University, E-29071, Málaga, Spain.

imf@ic.uma.es

Abstract: We study the effects of laser phase noise on a phase diversity coherent optical frequency domain (C-OFD) technique that has been recently proposed to measure passive devices used in dense wavelength division multiplexing (DWDM) systems. Theoretical expressions are provided to calculate the laser phase-noise to intensity-noise conversion in this technique under simplified circumstances. Obtained simulation results for a realistic measurement set-up show the validity of the approximate expressions. It is concluded that this effect is one of the limiting source of error for this measurement technique.

OCIS codes: (060.2300) Fiber measurements; (120.3180) Interferometry; (120.5050) Phase measurement; (230.3120) Integrated optics devices

References and Links

1. D. Derickson (ed), *Fiber optic test and measurement*, (Prentice Hall, Englewood Cliffs, N.J, 1998)
2. S. Kieckbusch, Ch. Knothe, and E. Brinkmeyer, "Fast and accurate characterization of fiber Bragg gratings with high spatial resolution and spectral resolution," in Proceedings of Optical Fiber Communication Conference (OFC2003), OSA Technical Digest Series (Optical Society of America, Washington, DC, 2003), pp. 379-381
3. M. Froggatt, J. Moore, T. Erdogan, "Full complex transmission and reflection characterization of a Bragg grating in a single laser sweep," in Proceedings of Optical Fiber Communication Conference (OFC2000), OSA Technical Digest Series (Optical Society America, Washington, D.C., 2000), pp. 22-24
4. G. D. VanWiggeren, A. R. Motamedi, and D. M. Baney, "Single-scan interferometric component analyzer," IEEE Photon. Technol. Lett. **15**, 263–265 (2003)
5. I. Molina-Fernandez et al, " Planar Ligthwave circuit six-port technique for optical measurements and characterizations," IEEE J. Lightwave Technol (to be published).
6. I.Molina-Fernández et al, "Coherent optical domain six-port measurement technique," in Proceedings of Optical Fiber Communication Conference (OFC2005), OSA Technical Digest Series (Optical Society of America, Washington, DC, 2005), paper OtuB2
7. G.F. Engen, "The six-port reflectometer: an alternative network analyser," IEEE Trans. Microw. Theor. Technol. **25**, 1075-1080 (1977)
8. S.O. Tatu, E. Moldovan, K. Wu, R.G. Bosisio, "A new direct millimeter-wave six-port receiver," IEEE Trans. Microw. Theor. Technol. **49**, 2517-2522 (2001)
9. F.M. Gannouchi and R.G. Bosisio, "A comparative worst-case error analysis of some proposed six-port designs," IEEE Trans. Instr. and Meas. **37**, 552-556 (1988)
10. G. F. Engen and C. A. Hoer, "Thru-reflect-line: an improved technique for calibrating the dual six-port automatic network analyzer," IEEE Trans. Microwave Theory Technol. **27**, 987–993 (1979)
11. G.F. Engen, "A least squares solution for use in the six-port measurement technique," IEEE Trans. Microw. Theor. Technol. **28**, 1473-1477 (1980)
12. M.Berman, P.I. Somlo and M.J. Buckley, "A comparative statistical study of some proposed six-port junction designs," IEEE Trans. Microw. Theor. Technol. **35**, 971-977 (1987)
13. P.B. Gallion et al., "Quantum phase noise and field correlation in single frequency semiconductor laser systems," IEEE J. Quantum Electron. **20**, 343-349 (1984)

#6580 - $15.00 US Received 10 February 2005; revised 15 March 2005; accepted 20 March 2005

14. A. Ortega-Moñux, I. Molina-Fernandez, J.G. Wangüemert-Perez, "Fourier Based Method-of-Lines Beam Propagation Method to analyse optical waveguide discontinuities," in *Procceedings of the 12th International Workshop on Optical Waveguide Theory and Numerical Modelling (OWTNM 2004)*, (Ghent, Belgium, 2004), pp. 43

1. Introduction

Dense wavelength division multiplexing (DWDM) system design puts stringent requirements in amplitude and phase response of passive devices (as, for example, arrayed waveguide gratings or fiber bragg gratings) which play a crucial role in these systems. Thus fast and accurate optical-domain measurement methods are been developed to substitute the traditional microwave-based indirect methods for optical device measurement. Coherent optical frequency-domain (C-OFD) techniques [1], such as coherent optical frequency-domain reflectometry (C-OFDR) [2], or swept frequency interferometry [3,4], are becoming increasingly important and they are competing with other optical domain techniques such as low coherence interferometry.

Recently a new phase diversity C-OFD technique has been proposed [5,6], with promising possibilities. This method is based in the six-port measurement technique, a well established and accurate method to measure complex reflection coefficients at microwave and millimeter-wave frequencies which is used by several metrological institutes to determine the complex reflection coefficient of commercial working standards [7], and that has also been recently proposed as a direct digital receiver [8]. Compared to other C-OFD techniques, which rely on frequency sweeping and interferogram demodulation, the six-port technique is intrinsically a single frequency technique, i.e. no sweeping of the laser source is necessary to completely determine the modulus and absolute phase of the reflection coefficient of the load at that specific frequency. This makes its precision basically dependent on the calibration process and not on the sweeping characteristics of the laser source. The core of the proposed technique is a small and rugged planar lightwave circuit (PLC) six-port junction, based on multi-mode interference (MMI) couplers, which was designed and simulated showing an excellent performance in a wide wavelength range. Although this germinal work has with no doubt open the possibility of extending the six-port measurement technique, so successful at microwave frequencies, up to the optical range, assessment of the optical six-port measurement technique as a whole, must still be carried out.

It is a well recognized fact that, aside from calibration errors, the accuracy of the six-port technique is determined by the power measurement errors [9]. Thus assessment of this technique at optical frequencies requires a careful study of the possible factors causing measuring errors at the four power detectors of the six-port setup. In doing so, special attention should be paid to those uncertainty mechanisms which are not encountered on microwave measurement setups and that, consequently, have not yet been quantified.

In this work the optical six-port technique is first briefly reviewed and the possible sources of power measurement errors are summarized and compared with those existing at microwave frequencies. From this analysis, optical coherence issues related to the laser phase noise (i.e., linewidth), appear as one of the main differences with the six-port microwave counterpart. Then the effects of laser phase noise on six-port power measurement errors is studied and simulated, and simplified expressions are obtained to calculate the power measurement uncertainties from the constituent parts of the setup.

2. The six-port measurement technique

Figure 1 shows the schematic of the proposed six-port optical reflectometer for measuring the complex reflection coefficient of a load (also known as device under test or DUT). The figure corresponds to a single polarization case. Of course, in a practical situation, polarization

#6580 - $15.00 US Received 10 February 2005; revised 15 March 2005; accepted 20 March 2005

related measurements would require additional hardware (polarization controller at the laser port and polarization diversity detection in each of the power meter outputs), but the study of phase noise effects can be carried out in a simpler manner based on this simplified single polarization assumption. The set-up is comprised of a narrow linewidth tunable laser source (TLS), a passive six-port junction, and four power meters (PM). The core of the measurement set-up is the passive six-port junction. This is a recently proposed [5,6], planar lightwave circuit (PLC) based on multimode interference couplers (MMIs) on a Δn=0.75% contrast Silica-on-Silicon buried channel waveguides technology. Although completely described in the aforementioned references, in Fig. 2 a schematic representation of the proposed six-port PLC is presented for the sake of completeness. It is basically composed of three interconnected MMI's: two identical 2x2 couplers (M_1 and M_2) and one 2x3 120º coupler (M_3). M_1 acts as a power divider; M_2 is used as a directional coupler, i.e. to separate the incident and reflected waves in the DUT and M_3 is the one in charged of setting the 120º phase difference between the three measurement signal at ports 3, 5 and 6, as required in a idealized six-port design [7]. The circuit schematic also contains two interconnecting waveguides W_D and W_C which are important in the six-port balance. TLS and PMs are considered to be high performance commercially available equipment. Interconnection between the different subsystems in the measurement set-up is done by short pieces of optical fibre, and low reflectivity connectors, such as straight PC ones (return losses better than -40 dB).

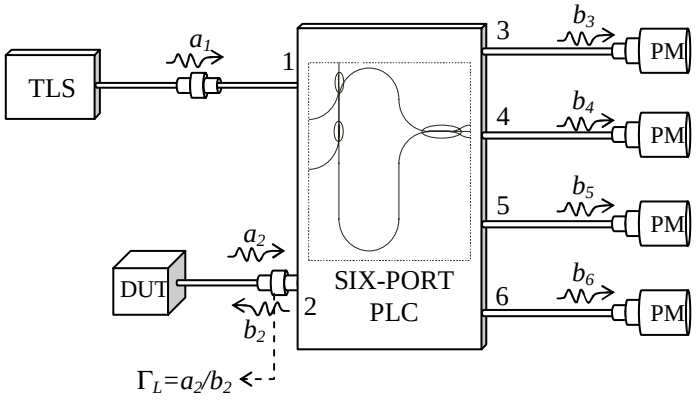

Fig. 1. Optical six-port measurement technique. Reflectometer set-up for complex reflection coefficient measurement

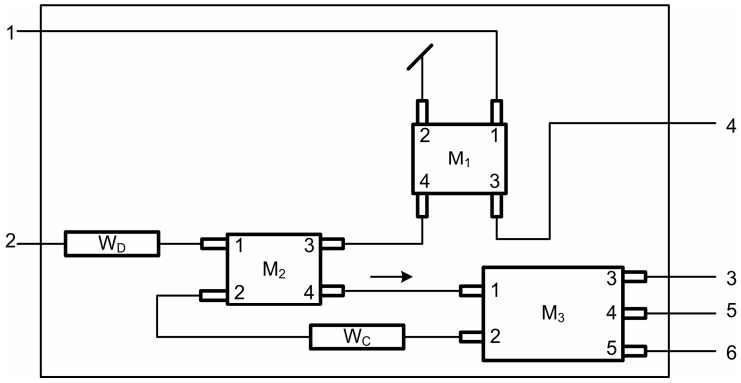

Fig. 2. Sixport planar lightwave circuit (PLC) architecture

#6580 - $15.00 US Received 10 February 2005; revised 15 March 2005; accepted 20 March 2005

The four PM readings can be calculated as [5],

$$P_i(\omega) = |b_2(\omega)|^2 \, K_i(\omega) \; \left| 1 - q_i^{-1}(\omega)\, \Gamma_L(\omega) \right|^2 \qquad i \in 3,...,6 \tag{1}$$

where, for a certain frequency ω, $K_i(\omega)$ and $q_i(\omega)$ are real and complex constant, respectively, which only depend on the six-port PLC and the reflection coefficient of the PMs (in real situations in which the PMs are well matched, these constants are almost completely determined by the six-port junction itself), $b_2(\omega)$ is the incident wave on the DUT, and $\Gamma_L(\omega) = a_2(\omega)/b_2(\omega)$ is the DUT reflection coefficient to be measured.

The complex values $q_i(\omega)$ play a crucial role in six-port theory. Six-port design goal is to get $q_4^{-1}(\omega) = 0$ (so that port 4 acts as a power reference port) and $q_3(\omega)$, $q_5(\omega)$, and $q_6(\omega)$ located symmetrically at 120º over a circumference of radius approximately equal to 1.5. These design values have shown to give the best accuracy for passive load measurement [7,12], under power measurement uncertainty. It has been demonstrated [5,6], that the proposed optical PLC approximately fulfils these design criteria in a great wavelength span of 100nm.

Normalizing power equations Eq. (1) with respect to the power of the reference port (habitually P_4) we come up with the three power ratio equations

$$p_i(\omega) = k_i(\omega) \frac{\left| 1 - q_i^{-1}(\omega)\Gamma_L(\omega) \right|^2}{\left| 1 - q_4^{-1}(\omega)\Gamma_L(\omega) \right|^2} \qquad i = 3,\ 5,\ 6 \tag{2}$$

where $p_i(\omega)=P_i(\omega)/P_4(\omega)$ and $k_i(\omega)=K_i(\omega)/K_4(\omega)$ which are the basis of six-port technique. For each frequency ω, Eq. (2) define three circles in the complex plane whose intersection is the reflection coefficient of the load $\Gamma_L(\omega)$. In these equations, there are four complex constants (q_3, q_4, q_5, and q_6) and three real constants (k_3, k_5,and k_6) which depend on the six-port junction and reflection coefficient of the PMs, but not of the load, that are determined by calibration [10].

3. Power measurement uncertainties

In practical situations, due to power measurement errors, the three circles defined by Eq. (2) will not intersect in a point, but still six-port theory provides an statistically quasi-optimum value for the unknown reflection coefficient Γ_L that can be estimated from the erroneous measurements [11,12]. It is a known fact [9], that these power measurement errors will, aside from calibration errors, determine the accuracy of the measurement technique. Thus, the causes of power measurement errors in the optical six-port set-up should be analyzed.

Main causes of power measurement errors in microwave six-port technique have been found to be related to thermal noise, zero drift, and nonlinearities [9], all of them directly linked to the PM performance. Possible effects due to the non-zero linewidth of the source have not been accounted for probably because, at microwave frequencies, the electrical size of the involved circuits is small, thus making this effects unimportant. At optical frequencies this assert no longer holds: the circuit size is typically several thousands of wavelengths long and finite coherence effects must be analyzed.

It must be noticed that, power measurement errors due to nonlinearity of the PMs are expected to be better at optical frequencies than at microwaves. Pin diodes, typically used as optical power sensing devices, are highly linear devices exhibiting dynamic ranges in excess of 60 dB, that are greater than their microwave counterparts, usually limited to approximately 50 dB (this is, for example, the case of Schottky diodes or thermocouples). In fact, it is usually recognized that optical PM nonlinearity is mainly due to the electronic circuitry that follows the photodetector, and not to the pin diode itself [1]. Of course this kind of nonlinearity is common to both optical and microwave setups.

#6580 - $15.00 US Received 10 February 2005; revised 15 March 2005; accepted 20 March 2005

On the other hand, power measurement noise sources can be divided into photodetector shot (quantum) noise and electronic noise. Electronic noise sources are thermal and low frequency flicker noise and are linked to the amplifier stages following the photodetector, thus being also common to microwave and optical setups. This noise levels do not depend on the received optical power and thus establish a noise floor at low received powers. On the contrary, shot noise, which increases with received power will be the limiting noise source at high optical levels. The effects of all these noise contributions can be easily calculated through well known expressions.

Besides this easily recognizable noise sources, there still exists another effect that is not so evident: it is the one that could follow from laser phase noise (related to the non-zero linewidth of the laser or, in other words, to finite coherence of the source) to intensity noise conversion. This is a well known effect that can be troublesome in C-OFDM techniques [1], and that is related to multiple reflections that cause different delayed optical signals to interfere with each other at the photoreceiver. The sixport technique being a phase diversity C-OFD technique in which each of the PMs (photodetectors) receives a combination, with different phases, of the two monochromatic waves to be compared (incident and reflected waves at the DUT) will with no doubt suffer from this detrimental effect.

4. Optical phase noise to intensity noise conversion in six-port measurement technique

4.1 Frequency domain interpretation of coherent homodyne detection

The influence of laser phase noise in coherent detection schemes, in which two optical beams interfere on a photodiode, has been analyzed in various situations including heterodyne and homodyne detection with different degrees of correlation between the interfering fields [13]. In that work, closed expressions were given for the power spectral density of the received photocurrent under the following approximations: a Lorentzian laser lineshape was assumed and only two incident waves, with certain relative level of delay (τ_0) and attenuation (α), were supposed to be present at the photodiode. Although it seems that no relation can be established between this simplified studies and the situation in the optical six-port, it will be shown that a close linkage exists among them. It must be realized that, phase noise to intensity noise conversion will happen whenever an optical noisy carrier passes through a linear system with frequency dependant amplitude response. In fact, from this point of view, the homodyne coherent detection scheme described in [13], in which a field and its delayed (τ_0) and attenuated (α) replica simultaneously impinge on a photodiode (with responsivity R), can be represented with the help of Fig. 3.

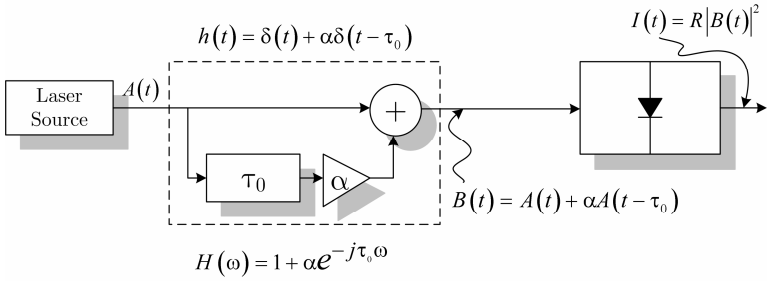

Fig. 3. Equivalent model for the homodyne coherent detection scheme

In this figure the laser output, which is modeled as a quasi-monochromatic amplitude-stabilized wave with random phase fluctuations

$$A(t) = A_0 \cdot e^{j[\omega_0 t + \phi(t)]} \tag{3}$$

#6580 - $15.00 US Received 10 February 2005; revised 15 March 2005; accepted 20 March 2005

is filtered by a linear time invariant (LTI) system with frequency response

$$H(\omega) = \mathrm{TF}\left[h(t)\right] = \mathrm{TF}\left[\delta(t) + \alpha\delta(t-\tau_0)\right] = 1 + \alpha\ e^{-j\tau_0\omega} \tag{4}$$

which represents the effect of interfering the two optical beams, a direct one and a delayed and attenuated replica, giving up to the interference field at the input of the photoreceiver

$$B(t) = h(t) * A(t) = A(t) + \alpha A(t-\tau_0)\,. \tag{5}$$

The laser output spectrum is of Lorentzian type, thus its power spectral density is given by

$$S_{AA}(\omega) = A_0^2 \frac{2\pi\Delta\nu}{(\pi\Delta\nu)^2 + (\omega-\omega_0)^2} \tag{6}$$

where $\Delta\nu$ is the full linewidth at half maximum (FWHM), ω_0 is the central angular frequency and A_0 is the amplitude of the laser source . Elementary LTI system theory dictates that the spectrum of the wave entering the photodiode will be given by

$$S_{BB}(\omega) = S_{AA}(\omega)\ \ \left|H(\omega)\right|^2 \tag{7}$$

The two sided spectrum of the detected photocurrent *I(t)* was calculated to be [13],

$$\frac{S_{II}(\omega)}{R^2 A_0^4} = \left[1 + \alpha^2 + 2\alpha\cos(\theta)e^{-\pi\bar{\tau}_0}\right]^2 \delta\left(\frac{\omega}{2\pi}\right) + \frac{4\alpha^2}{\pi\Delta\nu} e^{-2\pi\bar{\tau}_0} \frac{1}{1+\bar{\omega}^2} \times$$
$$\times\left\{\cosh(2\pi\bar{\tau}_0) - \cos(2\pi\bar{\tau}_0\bar{\omega}) + \cos^2(\theta)\left[\cos(2\pi\bar{\tau}_0\bar{\omega}) - \frac{\sin(2\pi\bar{\tau}_0\bar{\omega})}{\bar{\omega}} - e^{-2\pi\bar{\tau}_0}\right]\right\} \tag{8}$$

where $\theta = \omega_0\tau_0$, $\bar{\tau}_0 = \Delta\nu\tau_0$ and $\bar{\omega} = \omega/(2\pi\Delta\nu)$.

This filtering effect of the linear time invariant system is represented in Fig. 4 for a typical situation.

It can be seen that the ripple in the frequency response causes the spectrum of the optical field entering the photodiode to be distorted and this, once power detected, is converted into intensity noise. From this analysis it is clear that if the frequency response of the six-port setup (from the input laser port to any of the PM output ports) is somehow approximated, inside the spectral width of the laser source, in a way similar to that in Eq. (4), then the results in [13], (i.e. Eq. (8)) could be generalized to the six-port, and useful approximate expressions could be obtained to account for the phase noise to intensity noise conversion.

4.2. Phase noise to intensity noise conversion in the idealized six-port PLC

Microwave circuit theory shows that, if PMs are perfectly matched, optical fields on the four PMs can be calculated as

$$b_i(\omega) = \frac{S_{i1}(\omega)}{1 - S_{22}(\omega)\Gamma_L(\omega)}\left[1 - q_i^{-1}(\omega)\Gamma_L(\omega)\right]a_1(\omega) \qquad i = 3,4,5,6 \tag{9}$$

where $q_i^{-1}(\omega)$ reduces to

$$q_i^{-1}(\omega) = S_{22}(\omega) - \frac{S_{i2}(\omega)S_{21}(\omega)}{S_{i1}(\omega)} \qquad i = 3,4,5,6 \tag{10}$$

and $S_{ij}(\omega)$ are the scattering parameters of the six-port PLC. Furthermore, simulation results (obtained by means of a Bidirectional 3D-Scalar Method of Lines Beam Propagation Method

#6580 - $15.00 US Received 10 February 2005; revised 15 March 2005; accepted 20 March 2005

[14]) for the designed six-port PLC 5,6 show that internal reflections between the different discontinuities inside the circuit are very small and thus the following approximations can be done: a) $S_{22}(\omega)$ is always below –60dB ; b) $q_i(\omega)$ are slowly varying with ω; c) the modulus of $S_{i1}(\omega)$ is also a slowly varying function of ω , and its phase can be locally approximated by a line. Thus when applying (9) with $a_1(\omega)$ being the laser optical output centered at ω_0 and with a linewidth $\Delta\nu$ (typically below 10MHz) the following approximations hold

$$\left.\begin{aligned} & S_{22}(\omega) \approx 0 \\ & q_i^{-1}(\omega) \approx q_i^{-1}(\omega_0) \\ & S_{i1}(\omega) \approx S_{i1}(\omega_0)\ e^{-j\omega\tau_i(\omega_0)}, \quad \text{with} \quad \tau_i(\omega_0) = -\left.\frac{d\angle S_{i1}(\omega)}{d\omega}\right|_{\omega=\omega_0} \end{aligned}\right\} \quad i = 3,5,6 \quad (11)$$

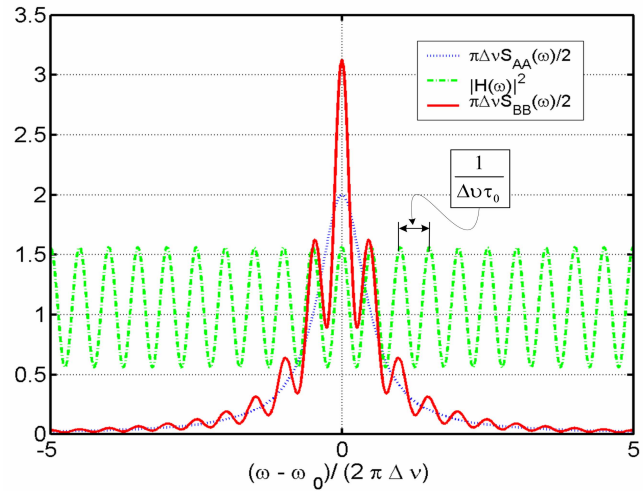

Fig. 4. Frequency domain representation of two optical beam interference spectrum at the photoreceiver input: $S_{AA}(\omega)$ laser spectrum, $S_{BB}(\omega)$ two optical beam interference spectrum at the photodiode input, $|H(\omega)|$ amplitude response due to the interference effect. Data: A_0=1.414 , Δν=10 MHz , τ_0= 200 ns , α=0.25 , $\omega_0\tau_0=2k\pi$

In Fig. 5 simulated results for these constants are presented showing that the aforementioned approximations are valid: Fig. 5(a) shows the $S_{2,2}$ modulus, Fig. 5(b) shows the evolution of the q_i points in the complex plane in a total frequency span of 125 GHz (1 nm) and Figs. 5(c) and 5(d) show, respectively, the modulus and phase of $S_{3,1}$ in the same frequency span. Insets are included in Figs. 5(c) and 5(d) showing the detailed behaviour in a reduced frequency span of ±10MHz correspondent to the maximum expected value of the laser linewidth. Although not plotted, for the sake of clarity, the same behaviour has been observed for the other S_{i1} parameters.

Putting these approximations into (9) the reduced expression

$$b_i(\omega) = S_{i1}(\omega_0)e^{-j\omega\tau_i(\omega_0)}\left[1 - q_i^{-1}(\omega_0)\Gamma_L(\omega)\right]a_1(\omega) \qquad i = 3,4,5,6 \qquad (12)$$

is obtained. The frequency response $H_i(\omega)$ from input port 1 to output port i (i=3,4,5,6) of the six-port can then be identified as

$$H_i(\omega) = S_{i1}(\omega_0)e^{-j\omega\tau_i(\omega_0)}\left[1 - q_i^{-1}(\omega_0)\Gamma_L(\omega)\right] \qquad i = 3,4,5,6 \qquad (13)$$

#6580 - $15.00 US
Received 10 February 2005; revised 15 March 2005; accepted 20 March 2005

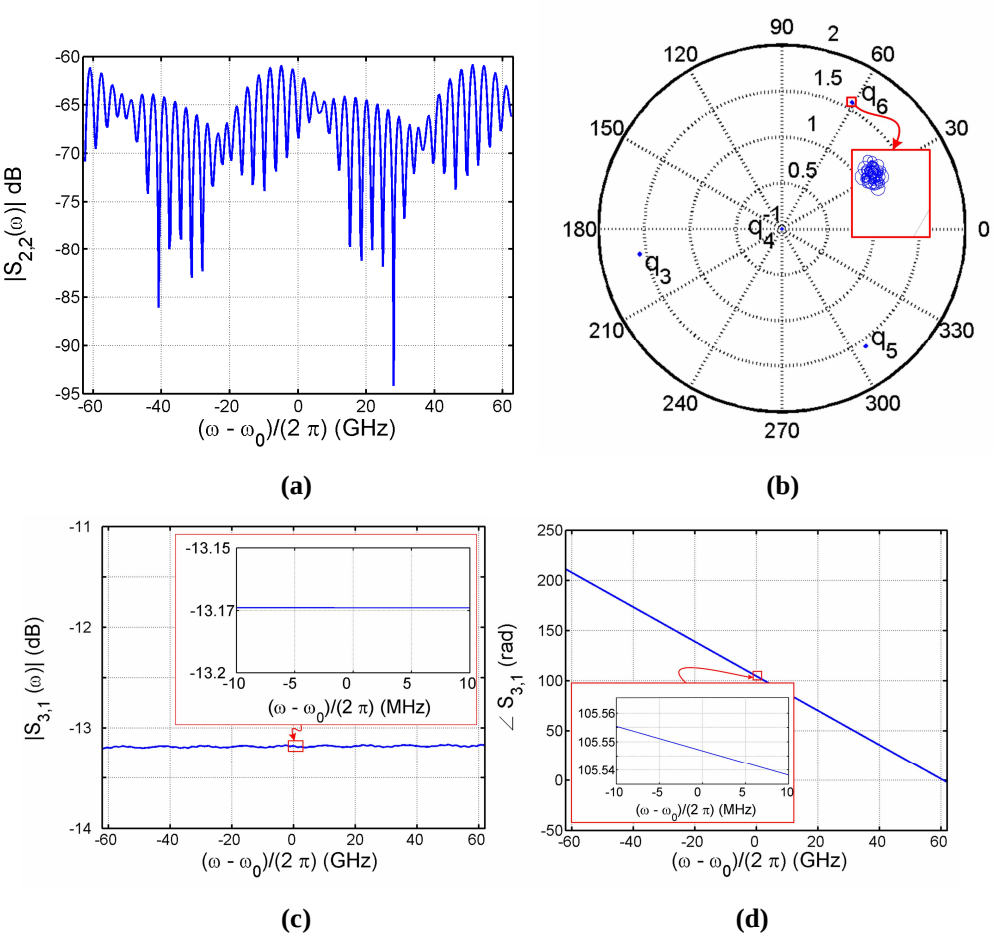

Fig. 5. Simulated frequency response of the optical six-port PLC. Simulation results have been calculated in 4000 frequency points in 1nm bandwidth centred at the laser central wavelength of 1550nm. The results shown in the insets of Fig. 5(c) and 5(d) have been calculated with a finer mesh of 4000 points in a ±10 MHz bandwidth around 1550nm.

It shows that, for the laser linewidth frequency scale, the effect of the idealized six-port junction is only to introduce a constant delay and attenuation, and thus the possible frequency domain ripple will only be due to the reflection coefficient of the DUT.

If the DUT is selected to be a perfect reflector at the end of a piece of idealized fiber (offset short), the reflection coefficient of the DUT will be

$$\Gamma_L(\omega) = -e^{-j2\tau_L\omega} \tag{14}$$

where τ_L is the one-way delay of the piece of fiber (related to its length by $\tau_L = (n_{eff}\, L_{DUT})/c$ where n_{eff} is the equivalent refractive index of the fiber and L_{DUT} the length of the fiber). Putting Eq. (14) into Eq. (13) yields

$$H_i(\omega) = S_{i1}(\omega_0)e^{-j\omega\tau_i(\omega_0)}\left[1+q_i^{-1}(\omega_0)e^{-j2\tau_L\omega}\right] \qquad i=3,4,5,6 \tag{15}$$

It must be noticed that Eq. (15) is identical to Eq. (4) when $\alpha = q_i^{-1}(\omega_0)$ and $\tau_0 = 2\tau_L$ (except for α being complex and for the constant scaling ($S_{i1}(\omega_0)$) and delay ($\tau_i(\omega_0)$) of the

#6580 - $15.00 US Received 10 February 2005; revised 15 March 2005; accepted 20 March 2005

preceding terms in (15)). Thus, under these approximations, Eq. (8) can be used to calculate the output photocurrent spectrum at the PMs of the six-port setup $S_{II,,i}(\omega)$ yielding

$$\frac{S_{II,i}(\omega)}{R^2 A_0^4 \left|S_{i1}(\omega_0)\right|^4} = \left[1+\left|q_i(\omega_0)\right|^{-2}+2\left|q_i(\omega_0)\right|^{-1}\cos(\theta_i)e^{-2\pi\bar{\tau}_L}\right]^2 \delta\left(\frac{\omega}{2\pi}\right)$$
$$+\frac{4\left|q_i(\omega_0)\right|^{-2}}{\pi\Delta\nu}\frac{e^{-4\pi\bar{\tau}_L}}{1+\bar{\omega}^2}\left\{\cosh(4\pi\bar{\tau}_L)-\cos(4\pi\bar{\tau}_L\bar{\omega})\right.$$
$$\left.+\cos^2(\theta_i)\left[\cos(4\pi\bar{\tau}_L\bar{\omega})-\frac{\sin(4\pi\bar{\tau}_L\bar{\omega})}{\bar{\omega}}-e^{-4\pi\bar{\tau}_L}\right]\right\} \quad (16)$$

where $\bar{\tau}_L=\Delta\nu\tau_L$ is the DUT-delay to laser-coherence time ratio, θ_i is now given by $\theta_i=\omega_0 2\tau_L-\angle q_i$, and the rest of parameters are defined as before. The first term in Eq. (16) is the squared DC photocurrent due to the beating between incident and reflected waves at the DUT (we will refer to it as $S_{II\_DC}=I^2_{DC}$, with I_{DC} being the DC photocurrent). It contains a exponential contrast loss term due to the finite coherence of the laser. The second term in Eq. (16) accounts for the phase noise to intensity noise conversion (it will we referred as S_{II_NOISE}).

In practical situations $\bar{\tau}_L<<1$ is a must for reduced contrast loss. Furthermore, the bandwidth of the electronic amplifiers, following the PM photodiodes, is sufficiently small so that in its pass-band the approximation $\bar{\omega}<<1$ holds. Then the intensity noise spectrum can be considered flat and Eq. (16) can be calculated as

$$\frac{S_{II,i}(\omega)}{R^2 A_0^4 \left|S_{i,1}(\omega_0)\right|^4} = \left[1+\left|q_i(\omega_0)\right|^{-2}+2\left|q_i(\omega_0)\right|^{-1}\cos(\theta_i)e^{-2\pi\bar{\tau}_L}\right]^2 \delta\left(\frac{\omega}{2\pi}\right)$$
$$+\frac{32\pi\left|q_i(\omega_0)\right|^{-2}}{\Delta\nu}\bar{\tau}_L{}^2 e^{-4\pi\bar{\tau}_L}\left[1-\cos^2(\theta_i)\right] \quad (17)$$

where the second term gives the photocurrent intensity-noise power density. Thus the relative intensity noise (RIN_i), due to the laser phase-noise to intensity-noise conversion at output port 'i', can be calculated as

$$\mathrm{RIN_i}(\mathrm{dB/Hz}) = 10\log\left(\frac{S_{II\_NOISE,i}}{S_{II\_DC,i}}\right) =$$
$$=10\log\left\{\frac{\frac{32\pi\left|q_i(\omega_0)\right|^{-2}}{\Delta\nu}\bar{\tau}_L{}^2 e^{-4\pi\bar{\tau}_L}\left[1-\cos^2(\theta_i)\right]}{\left[1+\left|q_i(\omega_0)\right|^{-2}+2\left|q_i(\omega_0)\right|^{-1}\cos(\theta_i)e^{-2\pi\bar{\tau}_L}\right]^2}\right\} \quad (18)$$

In the designed PLC $|q_i^{-1}(\omega_0)|$ is almost cero for the reference port 4, while it can be approximated by 0.6 for ports 3, 5 and 6 (see Fig 5(b)) in the analysed frequency span of 1nm. Thus the reference port will not suffer from phase noise conversion and, for the remaining ports, Eq. (18) shows that the RIN only depends on the DUT length through τ_L and θ_i.

#6580 - $15.00 US Received 10 February 2005; revised 15 March 2005; accepted 20 March 2005

5. Simulation results

In the previous section approximate analytical expressions where obtained to calculate the phase noise induced RIN in a PLC based six-port setup under idealized circumstances, i.e. perfectly matched PMs. In a real situation, PMs will not be perfectly matched and beating of incident and reflected waves on the interconnecting fibers will cause rapidly changing ripple in the frequency response which can increase the noise level.

To test the validity of the aforementioned approximations in a realistic situation a simulator has been developed to calculate the photocurrent power spectral density at the power detectors for the complete system of Fig. 3. The following procedure is applied: i) a realization of the laser source stochastic process is generated in the time domain as a quasi-monochromatic constant amplitude wave Eq. (3) with band-limited Gaussian random phase fluctuations corresponding to a Lorentzian spectrum (Eq. (6)) with spectral linewidth $\Delta\nu$; ii) this realization is then Fourier transformed to the frequency domain and filtered by the frequency responses $H_i(\omega)$ (i=3,4,5,6) of the complete six-port measurement set-up (including the possible beating due to incident and reflected waves in the interconnecting fibers and the response of the DUT) to get a realization of the wave entering the photodetectors in the frequency domain; iii) this is again transformed to the time domain and power detected to get the final photocurrent diode output whose power spectral density is then calculated. This process is repeated several times (N_{it}=300) and averaged to reduce the variance of the estimator and improve its quality.

The frequency responses of the system, from the laser input port to any of the PMs output $H_i(\omega)$, is calculated from the scattering parameters of the six-port PLC, those of the interconnecting devices (fibers, connectors…) and the frequency response of the DUT $\Gamma_L(\omega)$ by simple network analysis. Six-port junction PLC scattering parameters are obtained, as previously stated, by means of a Bidirectional 3D-Scalar Method of Lines Beam Propagation Method [14] which accounts for all the reflections in the different discontinuities of the PLC. The interconnection between the PLC and the power detectors have been modeled by pieces of standard fiber (n_{eff} = 1.5) of the same length (L_f=1m). Constant reflectivity (R_p = −40dB) connectors are inserted between the PLC and the fibers, simulating the pigtailing process. Also the PMs are simulated as constant reflectivity (R_{pm}= −40dB) blocks followed by a detector with unit responsivity (R=1A/W). A ideal reflector at the end of a piece of standard fiber, of length L_{DUT}, has been considered as the DUT for all the simulations. The laser source wavelength, linewidth, and power have been set to λ_0 = 1550 nm, $\Delta\nu$=100 KHz and A_0=0 dBm, respectively (corresponding to a high quality commercial tunable laser source).

Figure 6 shows, for two different DUT lengths, a comparison of the detected photocurrent noise power spectral density at port 5 ($S_{IL\_NOISE,5}$) obtained by simulation and evaluated by the analytical expressions obtained in previous section: the solid red curves correspond to analytical approximation (Eq. (16)) obtained when no reflections at the PM/PLC interconnection occur; the green dashed lines correspond to its narrow-band approximation (Eq. (17)); the dotted blue line are the simulation results obtained, as described in previous paragraph, for the complete system including the effects of the reflections in the PM/PLC interconnection. In this figure an excellent agreement between the theoretical curves, obtained in the previous section, and the simulation results is observed. Insets in Fig. 6 correspond to a narrower frequency span of 10 MHz (much greater than expected bandwidth of amplifier stages following the photodetectors) showing the validity of the narrow-band (flat spectrum) approximation Eq. (17). Similar results where obtained for the other measurement ports but they are not plotted for the sake of brevity.

#6580 - $15.00 US Received 10 February 2005; revised 15 March 2005; accepted 20 March 2005

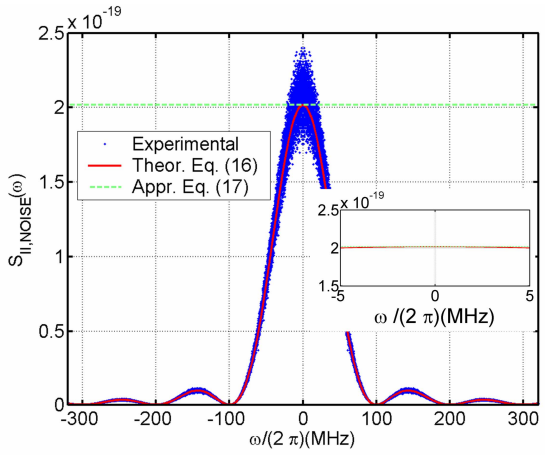

(a)

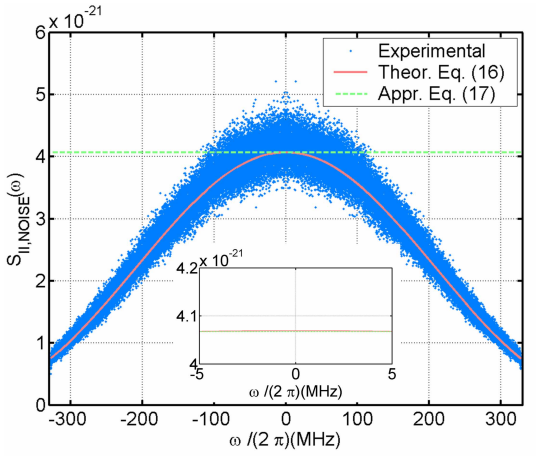

(b)

Fig. 6. Photocurrent noise power spectrum at port 5 ($S_{II\_NOISE,5}(\omega)$ (W/Hz)): a) L_{DUT} =1 m, b) L_{DUT} =0.2 m. Solid red lines show the theoretical spectrum calculated by Eq. (16), dashed green line show the narrow-band approach Eq. (17) and dotted blue lines show the simulation results for the complete system.

Once verified that the noise term of the photocurrent spectrum of Eq. (17) agrees with the simulation results, we should also confirm that the same its true for the DC part of this equation. Table 1 shows the comparison between simulated and theoretically predicted DC photocurrent (Eq. (17)) for measurement ports 3, 5 and 6, and for two different DUT lengths (L_{DUT} =0.2 m and L_{DUT} =1 m), showing also an excellent agreement.

Table 1: Theoretical (eq. (16)) and simulated results of the DC photocurrent in each measurement port.

Port	$S_{II\_DC,i}$ (dBmA) (Eq. (17))		$S_{II\_DC,i}$ (dBmA) (Simulated)	
	L_{DUT} =0.2m	L_{DUT} = 1m	L_{DUT} =0.2m	L_{DUT} = 1m
3	-26.30	-34.56	-26.39	-34.70
5	-32.92	-25.50	-32.90	-25.42
6	-18.16	-18.07	-18.07	-17.94

#6580 - $15.00 US Received 10 February 2005; revised 15 March 2005; accepted 20 March 2005

From Fig. 6 and Table 1, it is clear that Eq. (17) accurately predicts the complete photocurrent spectrum for different situations. Thus, Eq. (18) can be used to calculate the laser phase-noise induced RIN for the complete six-port measurement setup. This is done in Fig. 7 where phase-noise induced RIN (Eq. (18)) versus detected DC photocurrent (DC term of Eq. (17)) is plotted and compared with the shot and thermal noise RIN. These results correspond to port 5 and different DUT lengths, but similar results have been obtained for ports 3 and 6.

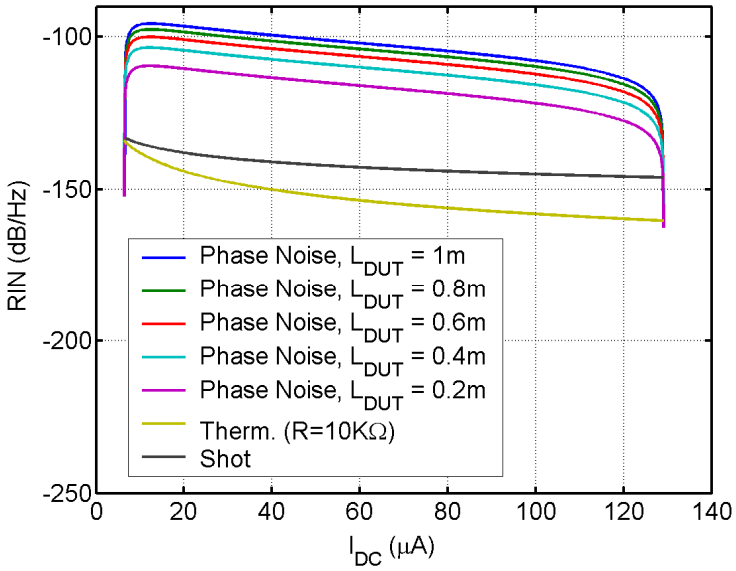

Fig. 7. Evaluation of phase-noise induced RIN versus DC photocurrent for different DUT lengths (port 5) and comparison with detector shot and thermal (noise equivalent resistance R=10 KΩ) noise.

From Fig. 7 it can be seen that for the analyzed example, laser phase-noise to intensity-noise conversion is the main source of power measurement errors, greatly exceeding the expected detrimental effects of other sources such as thermal or shot noise.

6. Conclusions

The influence of laser phase-noise to intensity-noise conversion has been studied in a recently proposed phase diversity C-OFD six-port measurement technique. Closed expressions have been developed to calculate the laser phase noise induced RIN at the four measurement PMs, based on simplified approximations. A stochastic simulator has been developed to simulate the complete system under realistic conditions. Simulation results show the validity of the aforementioned expressions. This study clearly shows that the laser phase-noise to intensity-noise conversion is the main source of power meter noise and thus this effect cannot be neglected when studying the performance of the six-port measurement technique at optical frequencies. Further studies must be carried out to quantify the consequences of this effect in the six-port calibration procedure and in the global accuracy of the measurement.

Acknowledgments

This work was supported by the Spanish MCYT under project TIC2003-07860. The authors wish to thanks Dr. Wangüemert-Pérez and Mr. Ortega-Moñux for their invaluable help in the development of the algorithms to simulate the PLC.

#6580 - $15.00 US Received 10 February 2005; revised 15 March 2005; accepted 20 March 2005